

our data with other experiments is satisfactory in the region of overlap. The disagreement among experiments at angles beyond 140° appears to exceed what might be expected from the standard deviations of the points.

Cross sections at small angles have been measured at other energies by experimenters at the General Electric Research Laboratory,²⁶ at M. I. T.,²⁷ and at the University of California.²⁸ Of these, final results are available at this time only for the California 260-Mev measurements, which indicate an angular distribution similar to that found in the present experiment.

VIII. CONCLUSIONS

We conclude that the angular distribution of positive photopions from hydrogen at 225-Mev photon energy is

²⁶ R. D. Miller and R. Littauer, *Bull. Am. Phys. Soc. Ser. II*, **2**, 6 (1957).

²⁷ B. Richter and L. S. Osborne (private communication to E. L. Goldwasser).

²⁸ Knapp, Imhof, Kenney, and Perez-Mendez, *Phys. Rev.* **107**, 323 (1957).

very satisfactorily described by the theory of Chew *et al.*, and cannot be fitted satisfactorily with a quadratic in $\cos\theta^*$. This constitutes direct evidence that the interaction of the photon with the meson cloud exists and has approximately the magnitude calculated by Chew *et al.*

IX. ACKNOWLEDGMENTS

The authors are grateful to Dr. R. C. Miller who actively collaborated in several phases of this work and to Dr. J. E. Leiss who made a number of the early tests of the short-pulse method. We are indebted to Professor G. Bernardini for helpful discussions. We wish to thank Mr. T. A. King and others of the betatron crew, who went out of their way to be helpful. Valuable contributions to the experiment were also made by Mrs. Dorothy Carlson-Lee and Lloyd Hendricks, Edward Eby, Donald Nigg, and Paul Baum.

Observation and Analysis of K^- Interactions*

J. HORNBOSTEL AND G. T. ZORN
Brookhaven National Laboratory, Upton, New York
(Received September 13, 1957)

In nuclear emulsions, 289 K^- mesons were observed. The mass and lifetime of K^- mesons is the same as that of K^+ mesons. The K^- mean free path in nuclear emulsion is geometric. Charge-exchange scattering and inelastic K^- -nucleus scattering are rare. Positive hyperons are emitted in 8% of K^- capture stars, negative hyperons in about 9%, hyperfragments in 5%. It is estimated that a Λ^0 is trapped without production of a visible hyperfragment in an additional 8%. A K^- is captured by one nucleon with formation of a Σ hyperon and a pion in about 0.77 of the cases, with creation of a Λ^0 and a pion in approximately 0.18 of the events. Capture by two nucleons occurs in roughly 0.05 of the cases. From a comparison of production and emission frequencies of Σ hyperons it is concluded that an attractive nuclear potential for Σ hyperons must be less than 20 Mev. Limits for the mean free paths for ordinary scattering, for charge-exchange scattering, and for absorption of Σ hyperons in nuclear matter are given. The trapping of Λ^0 hyperons in nuclei is discussed.

1. INTRODUCTION

IN continuing earlier studies¹ of K^- events observed in nuclear emulsions, 289 K^- mesons were found, most of them in stacks exposed at the Cosmotron. Analysis of this much enlarged sample (which includes the events of the previous study) made it possible to confirm or revise some of the earlier conclusions by basing them on statistically more reliable data, and to arrive at additional results relating to the behavior of hyperons in nuclear matter.

The presentation is divided into two essentially independent parts. The first deals with K^- interactions

in flight (Sec. 3) and with decays (Sec. 4). In the second, experimental data relating to K^- captures at rest are presented (Sec. 5) and analyzed (Secs. 6 and 7). In this analysis, use is made of experimentally determined relative frequencies of the three basic capture reactions of K^- mesons:

$$K^- + N \rightarrow \Sigma + \pi, \quad (\text{Ia})$$

$$K^- + N \rightarrow \Lambda^0 + \pi, \quad (\text{Ib})$$

$$K^- + 2N \rightarrow Y + N', \quad (\text{II})$$

where N and N' are nucleons and Y may be either a Σ hyperon (reaction IIa) or a Λ^0 (reaction IIb). Reactions (Ia) and (Ib) are referred to as mesonic, reaction (II) as nonmesonic captures. By comparing the reaction frequencies with the frequencies of observed charged Σ hyperons (corrected for inefficiency of de-

* Research carried out under the auspices of the U. S. Atomic Energy Commission.

¹ J. Hornbostel and E. O. Salant, *Phys. Rev.* **102**, 502 (1956); hereinafter referred to as HS I.

tection) and of hypernuclei—that is, of observed hyperfragments and of events in which a Λ^0 was captured in a nucleus without emission of a visible hyperfragment—information is obtained relating to the processes that can lead to trapping of hyperons in a nucleus.

2. EXPERIMENTAL TECHNIQUE

The methods employed in exposing the stacks, in processing and scanning the emulsions, and in analyzing the events were the same as the ones previously described.¹ Briefly, the stacks, each consisting typically of 36 G5 stripped emulsions, 2×3 in. in area and 400 μ thick, were exposed to a magnetically analyzed beam of negatively charged particles and were scanned near their leading edge for beam tracks of the grain density (about 2 times the minimum) expected for K^- mesons. A track so selected was followed to the point where the particle had decayed, interacted in flight, come to rest, or left the stack. A K^- meson could be immediately identified if it decayed, came to rest and made a star, or interacted in flight with production of an unstable particle. For other interactions in flight and for tracks that did not end in a star, the nature of the particle, pion, proton, or K^- , had to be determined by mass measurements. It is important to note that this procedure of scanning and measurement yields an unbiased sample of the K^- events.

Most K^- mesons were found in 12 fully or partly scanned stacks exposed at the Cosmotron when it was set to operate at 2.95 Bev. Under these conditions, the nominal K^- momentum was 340 Mev/c, except for the case of one larger stack, when it was 420 Mev/c. Several additional stacks were irradiated at lower Cosmotron energies (and somewhat lower beam momenta); in these exposures, the yield per stack of K^- mesons was reduced. One stack was exposed at the Bevatron to K^- mesons to 260 Mev/c. In it, 34 K^- mesons were found.

Except for the events previously reported on, no attempt was made to identify by multiple-scattering measurements nuclear particles ejected in K^- capture. Typical evaporation prongs were classified as protons, alpha particles, or fragments in the manner previously described.¹ For tracks ranging in density from 1.5 times the minimum to broken black, observation of the change in density with range made the assignment either to pions or to nuclear particles unambiguous in almost all cases. Tracks lighter than that, arising from K^- captures, were attributed to pions.

Kinetic energies T were determined from range, if the particle came to rest in the stack, and from ionization measurements, if it did not.

Lighter tracks were grain-counted. Each grain density g was normalized by reference to the density g_0 of beam pion tracks found in the immediate vicinity of the track to be measured. For each stack, the relationship between T/mc^2 (m =mass of the particle) and g/g_0 was established by grain-counting calibration

tracks. In some of the stacks, these were tracks of negative pions that stopped in the emulsions. Other stacks were exposed, in part of their area, to a beam of 80-Mev pions that traversed the emulsion at right angles to the main beam. (It was found that for $g/g_0 < 2$, the energy-grain-count calibration was within the limits of error independent of g_0 in the interval $g_0 = 20$ –35 grains/100 μ .) If tracks were too dense for grain counting, then the energy was estimated from gap measurements. In particular, this method was applied to most of the tracks of hyperons decaying in flight. In several cases, energies were confirmed by multiple-scattering measurements.

3. INTERACTIONS IN FLIGHT

3.1 Mean Free Path

K^- interactions in flight were systematically sought in 11 stacks. Only 1 out of 7 of the beam tracks followed was made by a K particle, the remainder being due to background protons. Consequently, the number of K^- mesons interacting in flight could be found only by determining for all interactions in flight the mass of the incoming particle by grain-count and multiple-scattering measurements. To provide sufficient track length for these measurements, events occurring within 1 cm from the leading edge of the emulsion were omitted from consideration. Tracks of identified K^- mesons coming to rest in the stack served for calibration.

To compute the mean free path, the total number of K^- mesons must be known, including those stopping without producing a star (K_p). Therefore, in 6 of the stacks, containing 112 stopping K particles, the fraction of K_p mesons was determined by measuring the mass of all particles stopping in the range interval in which K^- capture stars were found. This fraction was found to be 0.15 ± 0.03 . It was used to estimate the number of unidentified K_p mesons in the remaining stacks.

In the manner described, 44 K^- interactions in flight were identified in the 11 stacks. The corresponding total number of K^- mesons was $N_0 = 226$. The average range of stopping K particles was 5.55 cm. If (in addition to the interactions in the first cm) interactions occurring in the last 0.2 cm of range are also ignored² because in that interval it cannot always be decided whether the event occurred at rest or in flight, then the length of the average range interval in which interactions in flight are accepted is $x = 5.55 - 1.20 = 4.35$ cm. The corresponding energy interval is 15–100 Mev. Calculating the mean free path λ from the equation

$$N_0 - N_F = N_0 \exp(-x/\lambda), \quad (1)$$

where N_F is the number of interactions in flight, we obtain $\lambda = 20.4 \pm 3.0$ cm. The error represents the statistical fluctuation only.

² Actually, no interaction in flight was observed in which the K^- -track density near the event indicated a residual range ≤ 0.2 cm.

TABLE I. Number of elastic K^- -nucleus scatterings at residual ranges >1 cm.

	Observed	Calculated
$>10^\circ$	14	13
$>15^\circ$	7	8
$>20^\circ$	4	4

The geometric mean free path for emulsion is 25 cm. Correction for Coulomb attraction³ between the capturing nucleus and the K^- mesons, of average kinetic energy of 70 Mev, reduces this value to 22 cm, close to our measured mean free path. Fournet and Widgoff⁴ give $\lambda = (36.2_{-6.1}^{+9.2})$ cm, for essentially the same energy interval. We have no explanation for the discrepancy. Barkas *et al.*⁵ found $\lambda = 27.2 \pm 2.3$ cm.

The energy dependence of the mean free path is illustrated by the distribution in residual range of the interactions in flight, shown in Fig. 1. Individual events are indicated by dots near the base line. (The dots, but not the histogram, include 7 events, marked by vertical lines above the dots, found in the stacks which were not used for the determination of the mean free path.) A peak in the histogram is seen in the range interval between 2 and 3 cm which contains nearly one-half of the events. As other workers⁶ do not confirm such a peak, we must consider the irregularity to be the result of a chance fluctuation, although the probability of occurrence is less than 1%.

3.2 Charge-Exchange and Inelastic Scattering

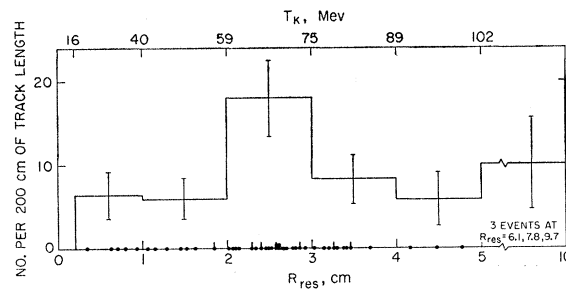
Charge-exchange scattering, that is conversion to \bar{K}^0 , could have occurred only in those interactions produced by K mesons in flight in which the visible energy E_{vis} is less than the kinetic energy T_K of the K mesons. Of the 44 interactions produced in flight, 11 meet this criterion. However, it is not excluded that a fraction F of these events are due to K^- absorption. This fraction can be estimated by a comparison with captures at rest, which frequently produce stars of low or vanishing visible energy. First it will be assumed that charge exchange at rest can be ignored. If one takes 30 Mev, which is slightly less than one half of the average kinetic energy of 70 Mev, as the portion of the kinetic energy appearing as visible star energy, then F can be equated to the fraction of stars produced at rest that have $E_{vis} \leq 70 - 30 = 40$ Mev. When K_p mesons are included, this fraction is observed to be 0.26, which leads to the expectation that $0.26 \times 44 = 11$ stars resulting from K^- capture in flight should be small enough to meet the energy criterion for charge-exchange scattering. Upon making alternatively the extreme assumption that all K_p events

³ R. M. Sternheimer, Phys. Rev. **101**, 384 (1956).

⁴ D. M. Fournet and M. Widgoff, Phys. Rev. **102**, 929 (1956).

⁵ Barkas, Dudziak, Giles, Heckman, Inman, Mason, Nickols, and Smith, Phys. Rev. **105**, 1417 (1957).

⁶ Private communications from W. H. Barkas and from R. S. White.

FIG. 1. Distribution in residual range of K^- interactions in flight.

are due to charge-exchange, it is found that 5 of the small stars produced in flight should be due to K^- absorption, leaving 6 stars attributable to charge-exchange scattering. Of course, the comparison with the observed number of 11 small stars is made uncertain by statistical fluctuations. Conservatively, it may be estimated that no more than one half of these 11 events, or about one-tenth of the interactions in flight, are actually due to charge-exchange scattering. Of course, in a K^- -nucleon collision the charge-exchange scattering could be appreciably more frequent, as in a nucleus a K meson (charged or neutral) can make several collisions, with the possibility of absorption in each of them.⁷

Only 3 of the 44 events are interpreted as inelastic K^- -nucleus scatterings. Thus, this process is infrequent. Again, it does not follow that K -nucleon scattering is also rare.⁸

3.3 Elastic Scatterings

As a K^- track was being followed, all deflections giving a change in projected angle $>5^\circ$ or a change in dip $>10^\circ$ were recorded. In no case was there a measureable change in grain density at the point of deflection, so that these events can be regarded to be elastic scatterings by nuclei. Scatterings by $\geq 10^\circ$ (spatial angle) occurring at residual ranges >1 cm are beyond the cutoff angle of Coulomb scattering and must, therefore, be nuclear. The number of these events is given in Table I. For comparison, expected numbers, calculated on the basis of an optical model,⁹ are also given. The experimental and calculated data are in good agreement.

3.4 K^- -Proton Interactions

Among the interactions produced in flight in a total path length of 1303 cm traversed by K^- mesons of from 16- to ~ 100 -Mev kinetic energy, there were two elastic

⁷ Alvarez, Bradner, Falk-Vairant, Gow, Rosenfeld, Solmitz, and Tripp, Nuovo cimento **5**, 1026 (1957), observing K^-p collisions in a bubble chamber, estimate that about 0.4 of the interactions in flight lead to charge exchange.

⁸ A survey of emulsion data gives a K^- -hydrogen scattering cross section of ~ 60 mb [M. Ceccarelli (private communication)]. A similar value was found by Alvarez *et al.* (see reference 7).

⁹ Fernbach, Serber, and Taylor, Phys. Rev. **75**, 1352 (1949).

TABLE II. K^- scatterings by free protons.

Event	Kinetic energies, Mev			K^- scattering angle, lab. system	Angle between primary K^- and proton	Coplanarity ^b	K^- scattering angle, c.m. system	K^- mass, m_e
	Primary K^- ^a	Secondary K^-	Proton					
164	58.8	14.1	44.7	98.8°	24.6°	0.1±0.6°	133°	960±7°
441	56.8	51.6	5.2	25.0°	75.2°	0.2±0.4°	39°	909±60 ^d

^a Calculated from energy balance.

^b Angle between incoming track and plane of outgoing tracks.

^c Calculated from ranges and included angle of outgoing tracks.

^d Calculated from ranges and from deflection of K^- .

scatterings by free protons. Data referring to these events are given in Table II. K^- masses calculated from the kinematics of the scattering agree with the τ^+ mass, $m_\tau = 966 m_e$,¹⁰ and with K^- mass values given by Gilbert *et al.*¹¹ (their most accurate value is $966.2 \pm 5 m_e$) and by Barkas *et al.*⁵ ($965.3 \pm 1.5 m_e$, $961.4 \pm 3.3 m_e$).

4. DECAYS

Of the K^- events occurring in flight, 8 were classified as decays. To be accepted in this class, an event had to meet two criteria. First, the appearance had to be consistent with a decay; especially, there could not be a blob at the junction of primary and secondary tracks. Second, the measurements of the tracks had to give results consistent with at least one of the established K^- -meson decay modes. Two events acceptable with regard to the first condition were rejected as decays because they failed to meet the second.

For the analysis, grain densities of primary and secondary tracks and, where feasible, the change in density with range and the multiple scattering of the secondary tracks were measured. If a track was not flat, then it was ascertained that distortion had not falsified the scattering results, for which purpose the distortion of steep tracks found in the vicinity of the track in question was examined.

Preferred identifications of the decays are given in Table III. In no case was it possible to establish the decay mode unambiguously.

From the number of decays and the total proper time of flight of all K^- mesons, of 8.4×10^{-8} sec, a mean life of $(1.1 \pm 0.4) \times 10^{-8}$ sec is calculated. This value agrees with the lifetime of K^+ mesons¹⁰ and with K^- lifetimes reported by Goldhaber *et al.*¹² [$(0.95_{-0.25}^{+0.36}) \times 10^{-8}$ sec] and by Barkas *et al.*⁵ [$(1.46_{-0.31}^{+0.38}) \times 10^{-8}$ sec].

5. K^- CAPTURES AT REST; EXPERIMENTAL RESULTS

We now turn to an analysis of K^- captures in nuclei and shall first present a classification of these events mainly with regard to the presence or absence of charged

hyperparticles, that is, of positive and negative Σ hyperons and of hypernuclei.

5.1 Classification of Events

In Table IV, the K^- captures at rest are grouped according to their characteristics. Observed numbers of events are entered in column III. Hyperons designated as Σ^\pm (line 3) decayed in flight into a pion.¹³ In columns III and IV, numbers followed by a question mark refer to cases in which the identification of a track as that of a hyperon was probable but not quite certain.

In one event, distinction between a decay in flight $\Sigma^+ \rightarrow p$ and a scattering of a proton was somewhat ambiguous. In two questionable Σ^- hyperons, a short track and a blob or Auger electron seen at the end of the presumed Σ track could have been coincidental. In one event,¹⁴ distinction between Σ^- and a hyperfragment was not possible; accordingly, this event was entered as ambiguous both in lines 4 and 8. In computing percentages, questionable events were given one-half weight. Of the hyperfragments, line 8, 3+1? made visible tracks, all but 1+1? less than 10μ long. In the remaining cases, the so-called double-centered events, the hyperfragment track was obscured by the blob found at the center of the K^- capture star, the presence of a double star being inferred from the failure of all star prongs to meet in one point.

The adjusted numbers and corresponding percentages, columns IV and V, were obtained as follows. (a) From the measured fraction of K_p mesons (0.15, see Sec. 3.1) it was estimated that 14 K_p mesons had been missed in those stacks, in which no systematic search for K_p mesons was made. The total number of K^- mesons (line 1) was accordingly increased. (b) From our observed average moderation times (4.6×10^{-11} sec for Σ^+ , 3.1×10^{-11} sec for Σ^-) and from the Σ^+ and Σ^- lifetimes,¹⁵ the expected numbers of Σ^+ and of Σ^- decays in flight was computed (9 $\Sigma^+ \rightarrow p$ or π , 4 Σ^-). Using this 9:4 ratio, 5 of the observed Σ^\pm hyperons were assigned to Σ^+ (line 5), 2 to Σ^- (line 6). (c) An appreciable fraction of Σ^- hyperons are captured without formation of a prong or emission of an Auger electron, and, therefore, escape detection. Fry *et al.*¹⁶ have estimated that 0.4 of all Σ^- captures at rest remain unidentified. From this fraction it is calculated that in our sample 8 Σ^- hyperons were missed. The number of Σ^- hyperons

¹⁰ A. M. Shapiro, Revs. Modern Phys. **28**, 164 (1956).

¹¹ Gilbert, Violet, and White, Phys. Rev. **103**, 248 and 1825 (1956).

¹² Iloff, Goldhaber, Goldhaber, Lannutti, Gilbert, Violet, White, Fournet, Pevsner, Ritson, and Widgoff, Phys. Rev. **102**, 927 (1956).

¹³ In $NK4$, the decay product was possible e^\pm ; see HS I.

¹⁴ $NK5$; see HS I.

¹⁵ See Alvarez *et al.*, reference 7.

¹⁶ Fry, Schneps, Snow, Swami, and Wold, Phys. Rev. **107**, 257 (1957).

TABLE III. K^- decays.

Event number	78	430	433	437	720	766	39a	B20
Preferred decay modes	$K_{\mu 2}$	$K_{e 3}$	$K_{\pi 2}$	$K_{\mu 3}$ $K_{e 3}$	$K_{\mu 2}$	$K_{\mu 2}$	no decision	$K_{\mu 3}$ $K_{e 3}$
Possible decay modes	$K_{\pi 2}$ $K_{\mu 3}$	$K_{\mu 2}$ $K_{\mu 3}$	$K_{\mu 2}$ $K_{\mu 3}$ $K_{e 3}$	$K_{\pi 2}$	$K_{\mu 3}$ $K_{e 3}$	$K_{\pi 2}$		$K_{\pi 2}$
Excluded decay modes	$K_{e 3}$	$K_{\pi 2}$		$K_{\mu 2}$	$K_{\pi 2}$	$K_{e 3}$		$K_{\mu 2}$

in column IV includes this correction, as well as the 2 above-mentioned decays in flight. (d) As, of the observed Σ^- hyperons, one-half were emitted in association with a pion, and one-half were unaccompanied by a pion (compare Table V), the data in column III, line 11 (events with pions but without hyperparticles, called group C in HS I) and line 12 (events without pions or hyperparticles, group D) were adjusted, to allow for the unidentified Σ_p hyperons, by subtracting 4 from each number. In addition, the 14 missed K_p mesons were added to group D. (e) The events entered in line 9 (and 10) are actually members of groups C or D which are not individually identified. Their number was estimated on the basis of the analysis given below in Sec. 5.4. No corresponding deduction was made in the numbers listed in the table for groups C and D.

5.2 Hyperon Events

Information relating to K^- captures with charged Σ emission is presented in Table V (5 K^- interactions in flight are included). Symbols are explained in the caption. The number of hyperons found is too small to allow statistically reliable conclusions with regard to their energy distribution, or to the characteristics of their decay and capture processes.

TABLE IV. Characteristics of K^- captures at rest.

I	II	III Observed No.	IV Adjusted ^a No.	V Percent
1	Total K^-	225	239	100
2	Σ^+	14+1 ?		
3	Σ^\pm	7		
4	Σ^-	11+3 ?		
5	Total Σ^+		19+1 ?	8±2
6	Total Σ^-		21+3 ?	9±2
7	Total $\Sigma^+ + \Sigma^-$		40+4 ?	17
8	Hyperfragments	12+1 ?	12+1 ?	5
9	Possible trapped Λ^0 's ^b		20±11	8
10	Hyperfragments+possible trapped Λ^0 's ^b		32+1 ?	14±4
11	With π , without hyperparticles (group C)	65	61	26
12	Without π or hyperparticles (group D)	112	122	51

^a See text for methods of adjustment.

^b Λ^0 's trapped in residual nucleus, or in hyperfragment of range too short for observation; see text for method of estimating number.

5.3 Visible Star Energies

The distribution in visible energy, E_{vis} , of stars resulting from K^- captures at rest is shown for events without hyperparticles in Fig. 2(A) and for events with charged hyperons in Fig. 2(B). E_{vis} was evaluated as outlined in Sec. 2 and in HS I. K_p captures, $E_{vis}=0$, are shown by a bar. Shaded areas refer to captures with pion emission, unshaded to those without pions. Events with pion tracks of dip (before processing) greater than 60° were not used for the plot, because kinetic energies derived from grain counts of such steep tracks are unreliable. In order not to distort the spectra, events with pions were given, in the plots, a weight inversely proportional to the fraction of events accepted [0.69 in Fig. 2(A), 0.87 in Fig. 2(B)].

It is seen that in about one-half of the events with charged hyperons, Fig. 2(B), the visible energy is close to the available energy of 494 Mev. (One event, shown above 500 Mev, has $E_{vis}=503\pm 10$ Mev, which is consistent with the available energy.) Two-thirds of the events of E_{vis} between 450 and 500 Mev have no prongs except those of the Σ and of the pion.¹⁷ Thus,

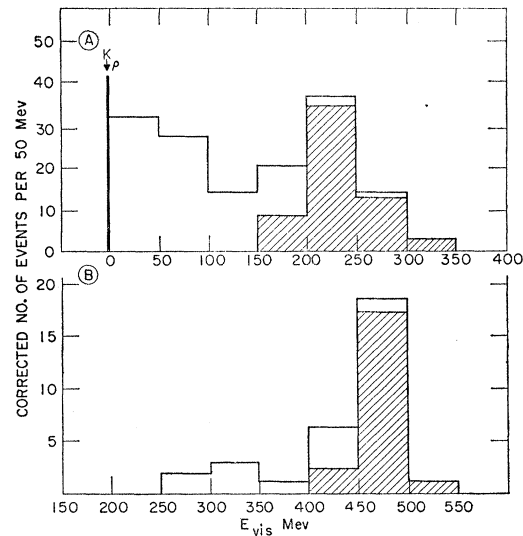


FIG. 2. Spectra of visible star energies. Histogram A for events without hyperparticles, histogram B for those with charged hyperons. Shaded areas refer to stars with a pion track.

¹⁷ This class was called Group A in HS I.

TABLE V. Data of events with hyperons. t_{flight} and t_{pot} are actual and potential hyperon flight times. ϑ' is the angle between directions of flight of Σ and decay pion in rest system of Σ . T_{Σ} and T_{π} are kinetic energies of Σ and of π , respectively, at emission. p_{res} and E_{vis} are the residual momentum and the visible energy of K^- star. In column 1, F denotes K^- interaction in flight. In column 2, F and R denote decays in flight or at rest, respectively; (?) means slight uncertainty whether F or R ; ? means stronger ambiguity. In column (11), (?) and ? have the same meaning with regard to the identification of the hyperon.

(1) Event	(2) Termination	(3) t_{flight} 10^{-11} sec	(4) t_{pot} 10^{-11} sec	(5) ϑ' degrees	(6) T_{Σ} Mev	(7) T_{π} Mev	(8) p_{res} Mev/c	(9) E_{vis} Mev	(10) Other prongs of K^- star ^a	(11) Comments
435	$\Sigma^+ \rightarrow p, R$	3.8		64	20	82 ± 10	211^b	503 ± 10	f	
606	p, R	2.6		100	14			275		
701	p, R	3.1		130	16			427	$140, p$	
508	p, R	12.0		112	49			330	$f_1; f$	React. II ?
311	p, F	1.5	2.5	95 (or 85)	14	$11(\pi^-)$	222^b	463	$12, p; 5, p$	
716	p, F				62			396	$10, \alpha; 29, p; f_1$? Or scattered p
8	π^+, R	1.7		170	10	66	60	476		
305	π^+, R	4.0		101	21	53	100	474		
B8	π^+, R	5.2		44	25	60	104	486		
422	π^+, R	3.5		20	18	47	155^b	466	f	
511	π^+, R	3.8		60	19	$35(\pi^-)$	114^b	492	$7, p; f; f_1$	
307	$\pi^+, R(?)$	3.3		145	18	45	227	464		
802	$\pi^+, R(?)$	15.3		55	30	57	240	488		
806	$\pi^+, R(?)$	1.6		31	12	$16(\pi^-)$	128	429		
B26	$\Sigma^{\pm} \rightarrow \pi^{\pm}, R?$	0.3		16	3	92	146	496		
73F	π^{\pm}, F	4.9	7.8	39	35	69	29^a	505		
1	$\pi^{\pm}, F(?)$	3.2	6.3^d	6	34	57	170	491		
229	π^{\pm}, F	3.8	6.8	30	31	22	192^b	495	$31, p$	
315	π^{\pm}, F	3.5	≤ 4.8	66	24			≤ 285		
B1	π^{\pm}, F	1.1	5.0	116	25			445	$120, p; 29, p$	
718F	π^{\pm}, F	8.7	12.7	31	51			408	$\{4, p; 43, p; 11, \alpha;$ $10, \alpha; f$	
B22	π^{\pm}, F	8.7	16.6	32	66		303^a	463	$126, p; f$	React. II
444	π^{\pm}, F	14.4	37.3	84	120			414	$9, \alpha; 14, \alpha;$	React. II
4	$e^{\pm?}, F$	4.9	6.0^d	125				406	$11, p$	React. II
226	$\Sigma^- \rightarrow 1$ prong + Auger	2.2			13	65	96	486		
308	2 prong	2.4			14	56	184	478		
B29	blob	2.1			12	154^f		574^f		
222	4μ prong	1.5			9	50	87	467		
500	1 prong	0.52			4	$34(\pi^-)$	136	446		
14F	2 prong	15.0			58	100	86^a	558		
25	2 prong + Yf^*	0.45			4			321	$10, p; 8, p; 8, p$	
150	3 prong	0.48			4			436	$154, p$	
704F	4 prong	4.1			21			289		
801	blob	4.3			21			361	$40, p; 12, p$	
51	clump + 12μ prong	3.7			9			324	$13, \alpha$	(?) clump + prong poss. accidental
601	Auger + 10μ prong	1.6			10	$46(\pi^+)$	100^b	480	$6, p$	(?) electron + prong poss. accidental
B19F	3 prong + f^a	1.4			9			301	$14, p$	(?) π^- or scattered K not excluded

^a f = tracks $< 10 \mu$ long; f_1 = tracks $10-29 \mu$ long.

^b Of Σ and π only.

^c Includes K momentum.

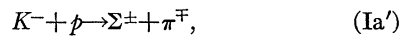
^d To end of stack. All others to end of residual range, within stack.

^e Of Σ and p only.

^f Values quite uncertain because of extreme steepness of pion track.

^{*} Yf = hyperfragment.

they illustrate the basic capture reaction



the effect of the binding of the proton in a nucleus appearing only in the energy and momentum balance of the events. In these cases, the residual momenta (p_{res} , see Table V) are of the order of magnitude of nucleon momenta and are, therefore, readily balanced by nuclear recoil.

The events without charged pions can be K^- captures with π^0 emission, nonmesonic captures (reaction II), or captures in which a charged pion is subsequently absorbed in the nucleus.

Figure 2(A) shows that in events without a charged hyperparticle (group C with π^{\pm} , group D without π^{\pm}) Λ^0 emission is energetically possible, as the visible energies do not exceed the limit above which a Λ^0 could not have been ejected, namely 307 Mev.¹ (The 2 events shown with $E_{\text{vis}} \geq 300$ Mev are no exceptions, as their visible energies are $E_{\text{vis}} = 300$ Mev and $E_{\text{vis}} = 320 \pm 50$ Mev.) Thus, the present more extended data confirm the conclusion of HS I that the energy balance of K^- capture is consistent with the theoretical postulate¹⁸ of

¹⁸ A. Pais, Phys. Rev. **86**, 663 (1952); M. Gell-Mann, Phys. Rev. **92**, 833 (1953); A. Pais, Physica **19**, 869 (1953); T. Nakano and K. Nishijima, Progr. Theoret. Phys. (Japan) **10**, 581 (1953);

conservation of strangeness. However, it does not follow—nor does the law of conservation of strangeness demand—that a Λ^0 actually emerged from all the stars of group C and D. On the contrary, it can be expected that in a number of events a Λ^0 was captured either in the residual nucleus, or in a fragment which could not be detected because of insufficient range. In the next section, an estimate of the frequency of such occurrences will be attempted.

5.4 Estimate of the Number of Unidentified Λ^0 Captures

In a subsequent section, we shall require an estimate of the number of all the Λ^0 hyperons trapped in the capturing nucleus. If a hyperfragment was formed but made a track so short (say $<0.5\mu$) that the two star centers cannot be resolved, or if the Λ^0 was retained in the residual nucleus, then the Λ^0 capture cannot be detected directly. An estimate of the frequency of these processes was obtained by comparing the visible-energy spectra of groups C and D with spectra derived for events in which a Λ^0 was trapped. For this purpose, the distribution in visible energy contributed by stable secondaries only, E_{vis}' , was studied. Except for the omission of the energy of unstable particles, E_{vis}' was evaluated with the conventions described before.

In events in which a Λ^0 is trapped, E_{vis}' will contain contributions from several processes.

(I) On the average, K^- captures will result in a nuclear excitation of 10–20 Mev,^{1,19} which can lead to production of evaporation prongs.

(II) Frequently, the pion (π^\pm or π^0) resulting from the K^- capture will in subsequent collisions transfer energy to the nucleus.

(III) If the Λ^0 results from the secondary reaction



then the nucleon N' , on the average of about 50-Mev kinetic energy, can directly (if a proton) or indirectly contribute to E_{vis}' .

(IV) Finally, the decay of the Λ^0 will liberate 176 Mev.

The spectrum of the portion of E_{vis}' resulting from processes (I) and (II) was taken to be the same as that of the observed E_{vis}' distribution of events in which a charged Σ was seen. If the Λ^0 results from reaction (A), then this is appropriate.²⁰ If, instead, the Λ^0 is formed in reaction (Ib), then, as can be easily seen, the contribution to E_{vis}' of process (II) may be underestimated,

M. Gell-Mann and A. Pais, *Proceedings of the 1954 Glasgow Conference on Nuclear and Meson Physics* (Pergamon Press, London, 1955); K. Nishijima, *Progr. Theoret. Physics (Japan)* **13**, 285 (1955); R. G. Sachs, *Phys. Rev.* **99**, 1573 (1955); M. Goldhaber, *Phys. Rev.* **101**, 433 (1956).

¹⁹ Gilbert, Violet, and White, *Phys. Rev.* **107**, 228 (1957).

²⁰We shall see below that the majority of Λ^0 's created in K^- captures do come from reaction (A).

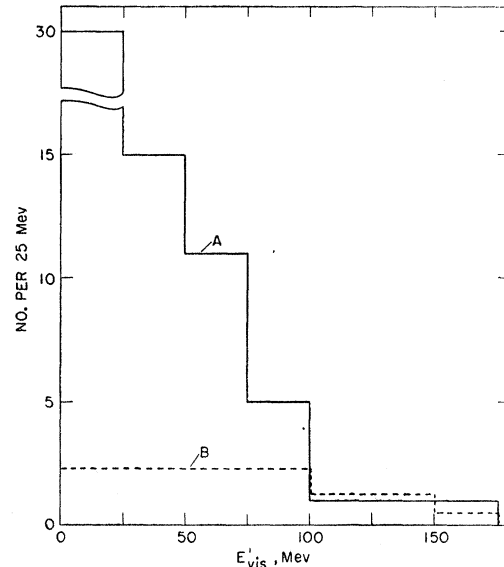


FIG. 3. Distribution in visible star energy of stable particles only for events with pions but without hyperparticles. Histogram A: observed distribution; histogram B: distribution expected for events in which a trapped Λ^0 decays.

because the pion is more energetic than a pion created in association with a Σ .²¹

Process (III) was ignored, which leads again to an underestimate of E_{vis}' .

The distribution of E_{vis}' in Λ^0 decay was taken from the work of Fry *et al.*²² For consistency, E_{vis}' was calculated from their data with our aforementioned conventions.

The distribution in star energy expected to be found in events in which a Λ^0 was trapped is obtained by folding the spectrum of processes (I), (II) into that of process (IV). The calculations were carried out separately for stars with and without pion emission.

The resultant spectra are shown in histograms B of Fig. 3 for events with pions, and in Fig. 4 for those without pions; they are superimposed on the histograms A representing the visible energy distributions of groups C and D. It is seen that histograms A and B differ in shape. The spectra A are peaked at energies below 100 Mev, whereas the spectra B are rather flat up to roughly 200 Mev. The estimate of the number of trapped Λ^0 hyperons was obtained by assuming that the high-energy tails of histograms A are due to events in which the decay of a trapped Λ^0 occurred. Accordingly, histogram B of Fig. 3 was normalized so that above 100 Mev the area under B equals that under A. Similarly, in Fig. 4 the areas above 125 Mev were made equal. With this normalization, the total area under A in Fig. 3 corresponds to 12 ± 7 events. (This number is statistically unreliable, as the normalization area under B contains only 3 events.) The total area of B in Fig. 4

²¹ See Table III of HS I.

²² Fry, Schneps, and Swami, *Phys. Rev.* **99**, 1561 (1955).

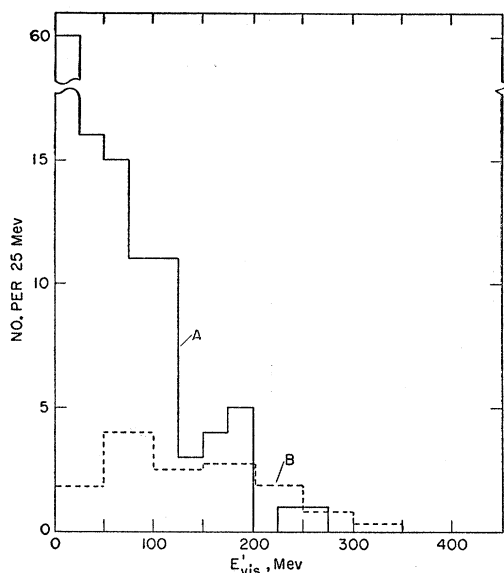
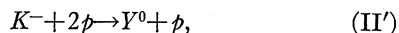


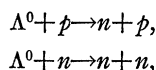
FIG. 4. Distribution in visible star energy of stable particles only, for events without pions or hyperparticles. Histogram A: observed distribution; histogram B: distribution expected for events in which a trapped Λ^0 decays.

corresponds to 28 ± 8 events. Thus, a total of 40 ± 11 events is assigned to trapped Λ^0 's.

This number, however, is an overestimate for the following reasons. (a) Our normalization procedure is equivalent to the assumption that in the absence of trapped Λ^0 hyperons the E_{vis}' spectra of groups C and D would be cut off sharply at 100 Mev and at 125 Mev, respectively. This is not likely to be the case. In group D, for instance, high values of E_{vis}' can also result if the K^- was captured by reaction (II'),



with the fast (~ 150 Mev) proton escaping. In fact, half of the events in the tail of histogram A, Fig. 4, owe their high energy to a proton of > 100 Mev, and could possibly contain examples of reaction (II'). (b) The contribution to E_{vis}' of process (III) was ignored. (c) The E_{vis}' spectrum of hyperfragments was taken from a sample of fragments of average $Z \approx 4$. If the nonmesonic²³ decay of the Λ^0 occurs by the reactions



then $\frac{3}{4}$ of the decay energy is transmitted to neutrons. In lighter elements, these neutrons will frequently escape; in heavier elements, as typified by residual nuclei of AgBr,²⁴ the energy will more often be redistributed in secondary collisions and in part be trans-

²³ In heavier elements, $Z \geq 3$, mesonic decay is rare.

²⁴ In making use in Sec. 7 of the results here obtained, it will be assumed that in three-quarters of the cases Λ^0 capture involves a heavy element.

ferred to protons, so that the fraction of the decay energy contributing to E_{vis}' will be closer to $\frac{1}{2}$.

The considerations of (b) and (c) show that the areas of histograms B above 100 Mev and 125 Mev, respectively, used in the normalization, actually represent a larger fraction of the total area than was estimated; consequently, the number of events corresponding to the area below these energies was overestimated.

A rough estimate of corrections *a*, *b*, and *c* leads to the conclusion, that the number of trapped Λ^0 's was overestimated by about a factor 2. Using, therefore, a correction factor 0.5 ± 0.25 , it is found that in $0.5 \times 40 = 20 \pm 11$ events a Λ^0 was trapped without formation of a visible hyperfragment. This number is entered in line 9 of Table IV.

5.5 Pion Spectra

Pion kinetic energies T_π were determined from grain counts. The pion energy distribution for events without hyperparticles (group C) is shown in Fig. 5(A), that for events with charged hyperons in Fig. 5(B). Pions from K^- interactions in flight are not included in the plots, nor are pion tracks of dip $\geq 60^\circ$. The median energy of the distribution of Fig. 5(B) is 55 Mev.

From reaction kinematics it follows that if the Fermi momenta of the capturing nucleons are taken to be less than 200 Mev/c, the pions created in reaction (Ia) have energies below ~ 90 Mev, pions from reaction (Ib) have energies ≥ 90 Mev.²⁵

The number of energetic pions allows, therefore, an estimate of the frequency of reaction (Ib). (Of course, pions of energy < 90 Mev can come from reaction (Ib), if they have lost energy in secondary collisions.) In the plot of Fig. 5(A), 7 pions have $T_\pi \geq 100$ Mev. Five tracks in the interval 75–100 Mev have individual energies of 85, 85, 87, 88, and 91 Mev, with an average error of ± 10 Mev; they could be due to either reaction. If these tracks are distributed between the parts of the spectrum below and above 90 Mev in proportion to the populations of the 50–75 Mev and the 100–125 Mev intervals, respectively, namely in the ratio 4:1, then a total of $1 + 7 = 8$ pions are assigned to reaction (Ib).

Several corrections must be applied before the frequency of reaction (Ib) is deduced. (a) The sample used for the plot contains only $\frac{2}{3}$ of all pions. (b) The pions must traverse nuclear matter before emerging. As their mean free path is short—their calculated median energy inside the nucleus is ~ 160 Mev,²⁶ not far from the

²⁵ HS I; Haskin, Bowen, and Schein, Phys. Rev. **103**, 1512 (1956). The values given in these papers were calculated by ignoring the effects of nuclear and Coulomb potentials. However, the effect of these potentials on the kinetic energies is small.

²⁶ In computing this energy, the pion-nucleus potential [R. M. Sternheimer, Phys. Rev. **101**, 384 (1956), and private communication] and the average nuclear excitation resulting from K^- capture by a bound nucleon (references 1 and 19) were taken into account. The number calculated in HS I without these corrections is slightly smaller than 160 Mev because it refers to the pion energy outside the nucleus.

resonance peak of π -nucleon scattering—a considerable fraction will collide and emerge with reduced energy. An estimate of the fraction g_2 of pions which will emerge with energies above 90 Mev was based on the measured pion-nucleon cross section (equal to $\frac{2}{3}$ the π^+p cross section),²⁷ on the angular distribution of the scattering process,²⁸ and on calculations, discussed in Sec. 6.3, of the relation between the mean free path in nuclear matter and the collision probability. For collisions resulting in a degradation of the pion energy below 90 Mev, a partial mean free path in nuclear matter of 1.3 times the geometric was found. To this value corresponds a fraction $g_2 \approx 0.3$.²⁹ (c) If emulsion nuclei are taken to consist of equal numbers of protons and neutrons, then it follows from charge independence³⁰ that the number of π^0 mesons from



is one-half the number of π^- mesons.

Applying the three corrections, the total number of pions, charged or neutral, created in reaction (Ib) is $\frac{3}{2} \times (1/0.3) \times \frac{3}{2} \times 8 = 60$. Thus, it is estimated that of the 239 K^- captures at rest, 25 \pm 9% occur according to reaction (Ib).³¹

This fraction may be compared with that derived from the data of Alvarez *et al.*³² who observed in K^-p captures the ratios $\Sigma^- : \Sigma^+ : \Sigma^0 : \Lambda^0 = 4 : 2 : 2 : 0.5$. By invoking charge independence, it is found that in self-conjugate nuclei reaction (Ib) should occur in 0.11 ± 0.03 (error statistical only) of all captures. In view of the large errors, there is no discrepancy between the two results. However, it is possible that the relative frequency of reactions (Ia) and (Ib) is actually different when the hyperons are created in K^- -hydrogen captures with the proton at rest, than when they are made in captures by nucleons moving within the nucleus.³² In a nucleus the distribution in hyperon energy may also be affected by the presence of discrete energy levels. This point will be considered more fully in Sec. 6.2.

²⁷ S. J. Lindenbaum and L. C. L. Yuan, Phys. Rev. **100**, 306 (1955).

²⁸ H. A. Bethe and F. de Hoffmann, *Mesons and Fields* (Row Peterson and Company, Evanston, 1955), Vol. II, Secs. 29d and 34c.

²⁹ See Fig. 11. The best value of the parameter d in Fig. 11 is between $0.1r$ and $0.2r$.

³⁰ Compare M. Koshiba, Nuovo cimento **4**, 357 (1956); S. Gasiorowicz, University of California Radiation Laboratory Report UCRL-3074 (unpublished).

³¹ Owing to a statistical fluctuation, the sample of K^- captures at rest analyzed in HS I contained a much larger proportion of fast pions than the present sample. Consequently, the frequency of reaction (Ib) was overestimated in the earlier publication.

³² Alvarez *et al.*, reference 7; also University of California Radiation Laboratory Report UCRL-3691, plus revised Table I (February 26, 1957); Falk-Vairant, Alvarez, Bradner, Gow, Rosenfeld, Solmitz, and Tripp, Bull. Am. Phys. Soc. Ser. II, **2**, 422 (1957); A. H. Rosenfeld (private communication). It should be noted that these ratios apply to K^- -hydrogen captures, where the relative kinetic energy of the K^- and the proton is zero. If these ratios are strongly energy dependent, then they may not apply to K^- captures by nucleons bound in a nucleus, where the nucleons, and possibly also the K^- , are not at rest.

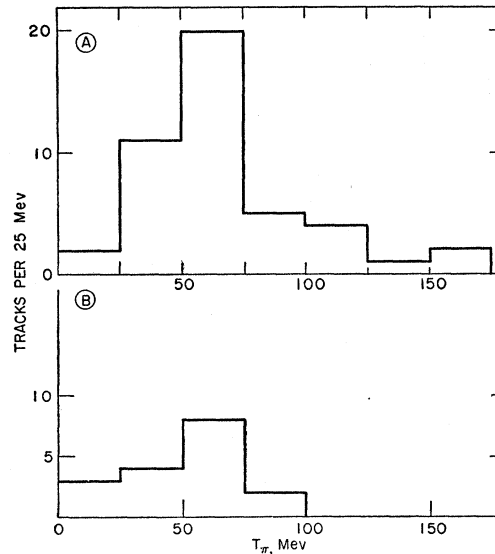


FIG. 5. Pion spectra. Histogram A for events without hyperparticles; histogram B for events with charged hyperons.

5.6 Nonmesonic K^- Capture

Nonmesonic K^- captures, resulting in the appearance of a charged Σ (reaction IIa) can be identified by the kinetic energy T_Σ of the Σ . The highest energy of a Σ from reaction (Ia) is about 45 Mev, whereas hyperons from reaction (IIa) have energies between ~ 30 and 180 Mev.²⁵ Accordingly, hyperons of kinetic energy ≥ 50 Mev were assigned to reaction (IIa). This limit excludes the minor interval below 50 Mev of the Σ spectrum of reaction (IIa), minor not only because its width is small but also because it represents a less populated tail of the spectrum.

In three stars, representing 1% of all K^- captures, such energetic Σ hyperons were observed (*NK* 4, 444, *B22*). If it is assumed that roughly one-half of the Σ hyperons either are absorbed or emerge with appreciably reduced energy, then this percentage must be doubled in order to obtain the fraction of charged hyperons produced in reaction (IIa). A further allowance must be made for Σ^0 hyperons. Assuming arbitrarily³³ that the number of Σ^0 hyperons does not much exceed that of charged hyperons, the total abundance of reaction (IIa) is $\lesssim 4\%$ of all K^- captures, and $\lesssim 5\%$ of captures leading to Σ formation (compare Sec. 6.1).

Nonmesonic capture may also result in the production of a Λ^0 (reaction IIb). Events involving this reaction cannot be identified; the only clue to its possible occurrence is the high kinetic energy of the nucleon emitted in association with the Λ^0 . This energy is between 70 and 250 Mev, with a median of about 170 Mev.³⁴ A

³³ For mesonic capture in self-conjugate nuclei it follows from charge independence, irrespective of the values of the matrix elements, that $(\Sigma^+ + \Sigma^-) : \Sigma^0 = 2 : 1$ (see reference 30). We were unable to find an equivalent theorem for the nonmesonic capture.

³⁴ Haskin, Bowen, and Schein, reference 25.

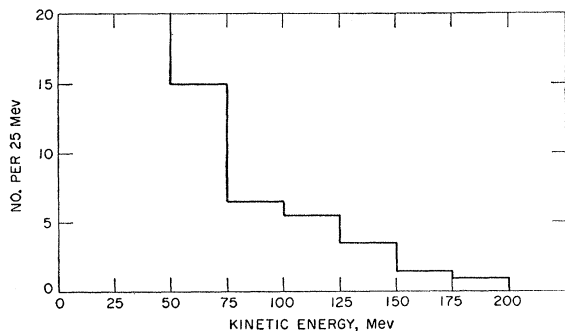


FIG. 6. Spectrum of protons emitted from K^- captures.

limit for the abundance of the reaction can be obtained by taking the number of protons with energies above 170 Mev, and doubling this number to allow for the lower half of the spectrum of reaction (IIb). From the spectrum of protons emitted from K^- stars, Fig. 6, one obtains in this way $2 \times 1\frac{1}{2} = 3$ possible examples of reaction (IIb). Correcting for energy losses of protons and for unobserved fast neutrons (combined factor 6), an estimate of 6% is obtained as a rough limit for the frequency of reaction (IIb). However, this number is not only statistically quite insecure, but the observed high-energy protons could have originated in other processes; for instance, in reaction (IIa) in association with a Σ^0 or with a Σ^- subsequently degraded or absorbed, or in the absorption of a fast pion. Indeed, the shape of the proton spectrum of Fig. 6 gives in itself no reason for the suspicion that the high-energy tail is not produced by the same processes, presumably pion interactions, which dominate below 170 Mev; it is incompatible with the interpretation that a large fraction of the protons below 170 Mev are due to reaction (II). It is therefore, entirely possible that the frequency of reaction (IIb) is much less than 6%.

In summary, it can only be said that the frequency of nonmesonic capture is low, of the order of 5%. Because of this infrequency, this reaction will be ignored in subsequent discussions.

On the basis of theoretical arguments, Cheston³⁵ deduced that in light nuclei approximately 20% of the K^- captures leading to Σ formation and 55% of the Λ^0 -producing captures should be nonmesonic. Cheston gives no corresponding estimate for heavy nuclei. If one assumes (a) that 0.4 of the K^- mesons interact with light nuclei,³⁶ and (b) that reaction (II) occurs quite infrequently in heavy nuclei, a lower limit of $0.4 \times 20\% = 8\%$ is obtained for the theoretical frequency of reaction (IIa). The experimental and theoretical numbers would agree, if we had overestimated the fraction of Σ hyperons which escape without appreciable energy losses and if assumption (b) is indeed valid. No cor-

³⁵ W. B. Cheston, Phys. Rev. **102**, 517 (1956).

³⁶ We take the relative capture probabilities of K^- mesons to be equal to those of μ^- mesons which were measured by H. Morinaga and W. F. Fry [Nuovo cimento **10**, 308 (1953)].

responding comparison can be made for reaction (IIb), mainly because this process is experimentally so poorly defined.

6. ABUNDANCE OF CHARGED Σ HYPERONS

6.1 Experimental Data

If we take the frequency of reaction (Ib) to be the average of the two quoted numbers 0.11 and 0.25, say 0.18, and accept 0.05 as an estimate for the abundance of reaction (II), then reaction (Ia) must have occurred in $1.00 - (0.18 + 0.05) = 0.77$ of all cases. The arguments to follow do not depend on the exact value of this frequency and are, therefore, not affected by the uncertainty in the abundance of reaction (Ib). If charge independence is valid, then charged hyperons are created in³⁸ $\frac{2}{3} \times 0.77 = 0.51$ of all captures. However, they were found to escape from the nucleus much less frequently, namely in 0.17 of the stars (see Table IV).

In order to be able to compare separately for Σ^+ and for Σ^- the fraction created with the fraction emerging, we again use charge independence. If we assume the results of Alvarez *et al.*³² to be independent of K^- energy and apply them to emulsion nuclei, it is found that negative and positive hyperons are created in the ratio $\Sigma^- : \Sigma^+ = (3.0 \pm 0.5) : 1$. Distributing the fraction 0.51 of all charged Σ 's accordingly, we find that a Σ^+ was made in 13% and a Σ^- in 38% of all K^- captures. The fraction observed is $7 \pm 2\%$ for Σ^+ and $8 \pm 2\%$ for Σ^- . Thus, the ratio of the number of hyperons observed to the number created is $\alpha^+ = 8/13 = 0.61 \pm 0.15$ for Σ^+ and $\alpha^- = 9/38 = 0.24 \pm 0.05$ for Σ^- .

A comparison with the results of other workers makes it likely that the above-given nominal values for the observed percentages of Σ , and consequently the nominal values of the quantities α , are more reliable than our large statistical error indicates. Fry *et al.*¹⁶ observed a Σ^+ in 6.1% of 1001 K^- stars plus an estimated³⁷ 170 K_p events, and a Σ^- in 7.3%. The latter number includes Σ^- decaying in flight into π^- , but excludes unidentified Σ_p^- , and is to be compared with our corresponding number of 6%. The uncertainty arising from the correction for Σ_p is common to both groups. The results of the European K^- Collaboration³⁸ appear to be similar: Σ^+ in 6.9% of 1800 stars, observed Σ^- in 7.8%.

6.2 Discussion of Model

In attempting to interpret the quantities α^\pm , it is easiest to base the analysis on an optical model and treat the production of hyperons in a nucleus and their possible subsequent interactions with nucleons essentially in the same manner as if the particles were free.

³⁷ Fry *et al.* used area scanning and, therefore, missed K_p endings. We used our K_p fraction to correct for this inefficiency. The Σ^+ and Σ^- fractions quoted in the text as results of Fry *et al.* include this correction.

³⁸ European K^- Stack Collaboration. C. C. Dilworth (private communication).

An obvious difference from the free-particle reactions results from the fact that the nucleons in a nucleus are not at rest. Consequently, hyperons created in reactions (I) do not have a unique kinetic energy, but a continuous spectrum of energies which is determined by the reaction kinematics. Scattering and absorption processes are similarly modified. (Changes in the kinetic energy of a nucleon are, of course, subject to the restrictions imposed by the exclusion principle.) In the model, the behavior of hyperons in nuclear matter is described by the three mean free paths λ_s , λ_{ce} , and λ_a for ordinary scattering, for charge-exchange scattering, and for absorption. These quantities are related to the corresponding cross sections σ_s , σ_{ce} , and σ_a by the well-known relation,

$$\lambda_i^{-1} = \rho \sigma_i, \quad (2)$$

where the subscript i stands for s , ce , or a , and ρ is the nucleon density. Furthermore, the average force between a hyperon and the nucleons is represented by a potential V which for charged particles is the sum of the Coulomb potential V_C and a nuclear potential V_N . (We shall take attractive potentials as positive.)

It is, however, not obvious that this model represents a good approximation of the actual situation, for the following reason. If the potential V is attractive, then, because of the finite nuclear size, there may exist discrete levels for hyperons of negative energy; in terms of the model this means that kinetic energies less than the well depth V cannot be continuously distributed. The model is, nevertheless, appropriate, if there are many closely spaced levels; but for moderate well depths this condition is not met. For instance, in a well 15 Mev deep and of the size of a silver nucleus, there are only about 10 levels³⁹ for a particle of spin $\frac{1}{2}$; in the light emulsion nuclei there exist under the same conditions only 1 or 2 levels. The number of levels increases rapidly with V .

For Σ hyperons, the width of these levels is likely to be large, because the hyperons will be destroyed in a short time, t , by the strong reaction



(N and N' stand for nucleons).⁴⁰ If we assume for t a rather large value, namely the transit time through a silver nucleus—this corresponds to a reaction cross section about one-tenth the geometric⁴¹—then the half-width \hbar/t of a level is about equal to the level spacing.

³⁹ H. Margenau, Phys. Rev. 46, 613 (1934).

⁴⁰ We are indebted to Dr. G. A. Snow for bringing this point to our attention.

⁴¹ Alvarez *et al.* (reference 7) observed the disappearance in flight of a Σ^- colliding with a proton. This may be an example of reaction (A), or it could be a charge-exchange scattering. We know of no other direct experimental evidence relating to the strength of reaction (A). *Note added in proof.*—Crawford, Cresti, Good, Gottstein, Solmitz, Stevenson, and Tycho [UCRL 3924 (unpublished)], recently observed two cases of Σ^+ production in Λ^0-p collisions. From their data and from the principle of detailed balancing it follows that the cross section for the inverse reaction, $\Sigma^+ + n \rightarrow \Lambda^0 + p$, must be of the order of the geometric cross section.

Under these conditions, the Σ spectrum is again continuous.

One obvious inadequacy of the optical model as applied to the analysis of the behavior of Σ hyperons in nuclei is, therefore, removed. In the remainder of this section, we shall assume the validity of the model, although we have been unable to estimate the effect of the finite nuclear size. (To the extent that the probability of creating Σ hyperons of kinetic energies less than V is not the same in K^- captures by bound and by free nucleons, the above-given ratio $\Sigma^-:\Sigma^+=3:1$ is inaccurate, because the Coulomb potential causes the well for Σ^- to be deeper than the well for Σ^+ .)

In the following calculations we shall also assume charge independence in strong reactions and ignore the small difference between the number of protons and of neutrons in emulsion nuclei.

6.3 Calculations

In the preceding, it was already implied that the following two mechanisms can prevent a hyperon from emerging from a nucleus. (a) A charged Σ may not reach the surface but may disappear in a collision with a nucleon, either by transformation into a Λ^0 in reaction (A), or by charge-exchange scattering. Of course, the latter process can also add to the supply of charged Σ 's through charge-exchange scattering of Σ^0 's. (b) If the hyperon within the nucleus finds itself in a potential well of depth V and has a kinetic energy T less than V , then, on reaching the surface, it will be unable to escape. Even if $T > V$, it may be retained by reflection at the nuclear surface. [Of course, if reaction (A) occurs at all, the trapped Σ 's will ultimately be converted into Λ^0 's.]

The quantities α^\pm are the product of two factors representing the two mechanisms: first, the proportion of Σ 's which arrive at the nuclear surface, and, second, the fraction of Σ 's that is able to leave the nucleus at the surface. The first factor is a function of the mean free paths in nuclear matter, λ_a , λ_s , and λ_{ce} ; the second factor depends on the Σ spectrum and on V . Of course, the shape of this spectrum is dependent on the probability of Σ -nucleon scattering, an effect which degrades the spectrum and thereby increases the fraction of Σ 's retained in a potential well. Moreover, as the probability of collision depends on the angle of emission (with respect to a nuclear radius vector), hyperons arriving at the surface at different angles will have been degraded in varying degrees. This complicates the calculation of the probability of reflection in the presence of scattering, because reflection and collision processes cannot be treated independently. Such calculations were not attempted.

The effect of charge-exchange scattering on the relative abundance of Σ^+ and Σ^- reaching the surface will be discussed later.

The following analysis was carried out in order to derive, by considering special cases, limits for the mean

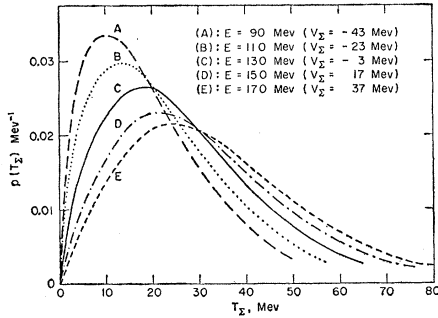


FIG. 7. Differential Σ spectra for various nuclear potentials V_Σ of Σ hyperons.

free paths and the nuclear potential of Σ hyperons from the values of α^+ and α^- . In this section we shall merely outline the assumptions made and the steps involved in the calculations. Mathematical detail is relegated to the Appendix.

First, the effect of a potential on the capture of hyperons will be calculated (mechanism b). Because of the Coulomb potential V_C , this effect is not the same for Σ^+ as for Σ^- . At the nuclear surface, the magnitude of V_C is about 3 Mev for light emulsion nuclei (C, N, O) and about 10 Mev for AgBr. For Σ^+ there exists a well within the nucleus, if $V_\Sigma > 0$; for Σ^- , if $V_\Sigma + V_C > 0$.

For Σ^+ , we shall ignore the barrier penetrability and set (for $V_\Sigma > 0$) the well depth $V = V_\Sigma$. As the penetrability becomes small about 3 Mev below the top of the barrier,⁴² a value of V_Σ determined from the Σ^+ -escape probability with this simplification will be too low by less than 3 Mev, an amount negligible compared to other uncertainties. For Σ^- , we have $V = V_C + V_\Sigma$.

The following considerations enter into the calculation of the fraction of unscattered Σ hyperons trapped in a well.

(a) The distribution in energy of Σ 's created by reaction (1a) in captures of K^- mesons by nucleons bound in a nucleus is obtained by an integration over

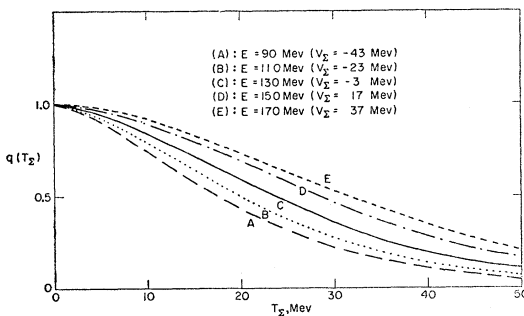


FIG. 8. Integral Σ spectra for various nuclear potentials V_Σ of Σ hyperons.

⁴² J. Mattauch and S. Fluegge, *Nuclear Physics Tables and Introduction to Nuclear Physics* (Interscience Publishers, Inc., New York, 1946), p. 66.

the nucleon-momentum spectrum, taken to be Gaussian with an average energy of 19 Mev,⁴³ and over the angle between the directions of motion of the Σ and of the nucleon. The energy E to be distributed between the reaction products is given by

$$E = Q_0 - V_N + T_F + V_\Sigma + V_\pi + V_C \equiv E_1 + V_\Sigma,$$

where $Q_0 = 100$ Mev is the Q of the free reactions,⁴⁴ V_N is the nuclear potential and T_F the kinetic energy of the nucleon (on the average $-V_N + T_F \approx -20$ Mev),⁴⁵ V_Σ is defined as before, V_π is the pion potential, $V_\pi = 46$ Mev,⁴⁶ and V_C was taken as +7 Mev, an average for light and heavy nuclei; E_1 is defined by the equation. E is independent of a possible K^- nuclear potential V_K . The computations were carried out for various assumed values of V_Σ . It turns out that the shape of the spectrum is not sensitive to the precise value of E (compare the various curves in Fig. 7).

(b) As the value of V_K is unknown,⁴⁷ we set $V_K + V_C = 0$. (We shall return to this point.) Then the K^- kinetic energy T_K in the nucleus (for captures at rest) is also zero.

(c) It was assumed that the capture reaction is isotropic in the center-of-mass system⁴⁸ and has an energy-independent cross section. The resultant differential spectra $p(T_\Sigma)$, calculated for several values of V_Σ , are shown in Fig. 7. The corresponding integral spectra,

$$q(T_\Sigma) = \int_{T_\Sigma}^{\infty} p(T) dT,$$

are plotted in Fig. 8. The fraction of Σ 's having insufficient energy to escape from a potential well of depth V is

$$f_{i\Sigma} = 1 - q(V). \quad (3)$$

$f_{i\Sigma}$ is found as a function of V_Σ by taking $q(V)$ from the spectrum calculated for $E = E_1 + V_\Sigma$, and using $V = V_\Sigma$ for Σ^+ , $V = V_\Sigma + V_C$ for Σ^- ; the relationship is displayed in Fig. 9. To find the curve for Σ^- , it was assumed that 0.4 of the K^- captures occur in the light emulsion nuclei ($V_C = 3$ Mev) and 0.6 in AgBr ($V_C = 10$ Mev).⁴⁶

⁴³ E. M. Henley and R. H. Huddleston, *Phys. Rev.* **82**, 754 (1951).

⁴⁴ This is an average for Σ^+ and Σ^- . The small difference in Q_0 for Σ^+ and Σ^- can here be neglected.

⁴⁵ Obtained with $V_N = -35$ Mev and with the median of T_F , $\bar{T}_F = 15$ Mev. The quantity $-V_N + T_F$ also equals the sum of the nucleon binding energy and the average nuclear excitation in K^- capture, for which Gilbert *et al.* (reference 19) also give a value of -20 Mev.

⁴⁶ R. M. Sternheimer (see reference 26). V_π depends rather strongly on the pion energy. The quoted value corresponds to the observed average kinetic energy of 60 Mev of pions emitted in association with a charged Σ .

⁴⁷ A tentative value was deduced by M. Ceccarelli (private communication).

⁴⁸ This assumption is not necessarily valid, as typical Fermi energies, say $T_F = 15$ Mev, are large enough so that p states could be important.

Because of the effect of the Coulomb potential, $f_{i\Sigma}$ is larger for negative than for positive hyperons.

If $V_K > 0$, $T_K > 0$, then the relative motion between the K^- and the nucleon is increased and the spectrum will be broadened. This will cause a steeper rise of the curves in Fig. 7 near $T_\Sigma = 0$, a more gradual fall for large T_Σ , and a reduction in height of the peak. Presumably, for a given value of V_Σ , $f_{i\Sigma}$ (and the fraction reflected, $f_{r\Sigma}$, referred to below) would be increased.

(d) Hyperons having kinetic energies greater than the well depth V may still be retained in the nucleus by reflection at the boundary. The fraction reflected, $f_{r\Sigma}$, will be calculated under the assumption that scattering is negligible.

If particles of energy $T_\Sigma > V$ are emitted isotropically from a point located a distance d from the surface of a nucleus of radius r , then the fraction R totally reflected by a potential step of height V near the surface is (see Appendix)

$$R = \left[1 - \frac{1-w}{(1-\delta)^2} \right]^{\frac{1}{2}}, \quad (4)$$

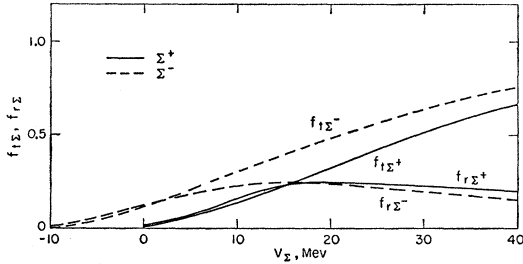


FIG. 9. Probabilities of trapping, $f_{i\Sigma}$, and of reflection, $f_{r\Sigma}$, of Σ hyperons in a well, as a function of the nuclear potential V_Σ .

where $w = V/T$ and $\delta = d/r$. (We again take a potential barrier as impenetrable.) The equation is valid for $T < T_1$, where $T_1 = V/[1 - (1-\delta)^2]$. For $T > T_1$, one has $R = 0$. There is also *partial* reflection at angles of incidence φ less than the angle of total reflection φ_t . However, the reflectivity falls rapidly to low values for $\varphi < \varphi_t$, especially if the change in potential is gradual; hence this effect can be neglected.

The reflected fraction $f_{r\Sigma}$ is obtained by averaging R over the Σ spectrum $p(T_\Sigma)$; it is, of course, a function of δ , increasing with decreasing δ . In principle, therefore, $f_{r\Sigma}$ should be averaged over the nuclear volume. But as the distribution of the points of K^- capture is not known, $f_{r\Sigma}$ was, instead, calculated for the median value, 0.2, of δ which one would obtain if these points were uniformly distributed over the nucleus. Actually, a somewhat smaller value might give a better approximation, as, due to the strong interaction of K^- mesons (see Sec. 3.1), the capture points will be concentrated near the nuclear surface. For instance, for a density of these points proportional to $\exp(-d/\lambda_{\text{geom}})$ (λ_{geom} is the geometric mean free path in nuclear matter), one

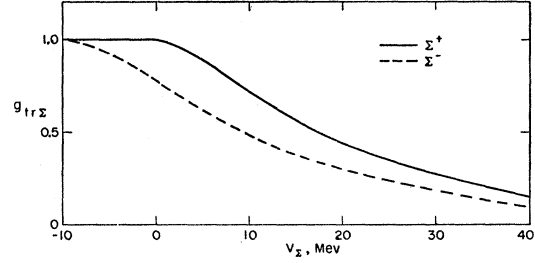


FIG. 10. Probabilities of escape of Σ hyperons from a well, as a function of the nuclear potential V_Σ .

calculates for AgBr a median of δ equal to 0.1. Fortunately, it turns out that the results of the analysis depend only weakly on the choice of δ .

In expressing $f_{r\Sigma}$ as a function of V_Σ , the considerations mentioned in connection with Eq. (3) apply. The function is plotted in Fig. 9.

Of the Σ 's reaching the nuclear surface without a collision, the fraction that will escape is $g_{tr\Sigma} = 1 - (f_{i\Sigma} + f_{r\Sigma})$. In Fig. 10 the relation between $g_{tr\Sigma}$ and V_Σ is shown. Had we chosen a smaller value of δ , then the fraction escaping would have been less. For instance, for Σ^- and $V_\Sigma = 0$, $g_{tr\Sigma^-} = 0.78$ for $\delta = 0.2$, and $g_{tr\Sigma^-} = 0.67$ for $\delta = 0.1$. Conversely, for $\delta = 0.2$, the value $g_{tr\Sigma^-} = 0.67$ corresponds to $V_\Sigma = 3$ Mev; thus, it is seen that a considerable change in δ is equivalent to a small change in V_Σ .

(e) The other factor, mentioned before, which affects the hyperon escape probability, is the fraction g_i of particles that reach the surface of emulsion nuclei without interacting. In Fig. 11, g_i is shown as a function of $\lambda/\lambda_{\text{geom}}$ for several values of δ (see Appendix for calculations).⁴⁹ It is seen that the curves for $\delta = 0.2$ and $\delta = 0.1$ are similar; only for still smaller values of δ is g_i appreciably decreased.

6.4 Discussion

To fit the observed quantities, $\alpha^+ = 0.61$ and $\alpha^- = 0.24$, four parameters can be suitably selected, namely V_Σ

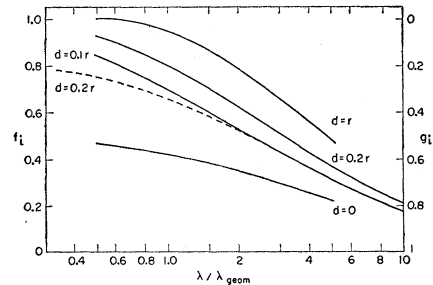


FIG. 11. Probabilities of collision f_i of particles created in an emulsion nucleus of radius r at various distances d from the surface; $g_i = 1 - f_i$.

⁴⁹ λ_{geom} was computed from Eq. (2), with $\sigma_{\text{geom}} = \pi(\hbar/m\pi c)^2$ and $\rho^{-1} = (4\pi/3) \times 2.0 \times 10^{-39}$ cm³. This density corresponds to the nuclear radii found by R. Hofstadter [Revs. Modern Phys. 28, 214 (1956)].

and the mean free paths for ordinary scattering, for charge-exchange scattering, and for absorption. However, they cannot be determined unambiguously from the data. Furthermore, as mentioned before, the trapping fraction was not computed for Σ 's which have been scattered. We shall, therefore, investigate simplified cases.

(I) If nuclear interactions of Σ 's are ignored, that is, if we set $\lambda_a = \lambda_s = \lambda_{ce} = \infty$, then $g_i = 1$ and an upper limit is obtained for the fraction escaping from a nucleus of well depth V , namely, $\alpha = g_{tr\Sigma}$. From Fig. 10 it is seen that the value $\alpha^+ = 0.61 \pm 0.15$ requires that V_Σ be limited to ≤ 20 Mev. The limit similarly derived from α^- is less restrictive, namely 30 Mev. The smaller of the two limits, 20 Mev, could not be much increased, even if the $\Sigma^- : \Sigma^+$ production ratio of 3:1 derived from the data of Alvarez *et al.*³² were not applicable in our case. Assuming, for instance, $\Sigma^- : \Sigma^+ = 2:2$, one gets $\alpha^- = 0.36 \pm 0.07$ and $\alpha^+ = 0.30 \pm 0.07$, corresponding to 20 Mev and 35 Mev, respectively. Thus, the more restrictive limit is the same as before. The highest limit, 26 Mev, is obtained for $\Sigma^- : \Sigma^+ = 2.5:1.5$. These conclusions are relatively little affected by the limitations of the model, as the number of levels is fairly large if $V_\Sigma > 20$ Mev.

Of course, if λ_s is such that g_i is appreciably less than 1, then the limits for V_Σ are lowered. The same comment applies to λ_{ce} , as will be discussed below.

(II) If charge-exchange scattering is unimportant, so that the $\Sigma^+ : \Sigma^-$ ratio of hyperons arriving at the surface is the same as that at production, namely 3:1, then a *lower* limit for V_Σ can be set from the observation that α^+ is much larger than α^- . As g_i is charge independent, and as for $V_\Sigma < -10$ Mev all particles reaching the surface, Σ^- as well as Σ^+ , can escape, one would expect in this case $\alpha^+ = \alpha^-$. It, therefore, follows that $V_\Sigma > -10$ Mev.

(III) From Fig. 10 it can be seen that for any value of V_Σ , $g_{tr\Sigma^+} / g_{tr\Sigma^-} \lesssim 1.5$, appreciably less than α^+ / α^- . The observed ratio $\alpha^+ / \alpha^- = 2.5$ can be explained, if it is assumed that an appreciable portion of the Σ 's reach the surface only after having been scattered. As scattering produces a degradation of the spectrum, it is clear that for scattered Σ 's the effect of the Coulomb potential, and thereby the difference between the trapping of Σ^- and of Σ^+ , is enhanced.

A rough estimate of the effect of scattering was based on a crude approximation in which it was assumed that in each scattering process a hyperon loses one-half its kinetic energy. It was found that for the so-obtained spectrum of scattered hyperons the ratio of the escape probabilities $g_{tr\Sigma^+} / g_{tr\Sigma^-}$ of Σ^+ and Σ^- is about 2 for $0 \leq V_\Sigma \leq 15$ Mev, in better accord with the observed $\alpha^+ : \alpha^-$ ratio. Furthermore, if absorption and charge-exchange scattering were negligible and if the Σ 's would reach the surface after one collision, then the observed values of α^+ and α^- would require $V_\Sigma \approx 8$ Mev.

In order that an appreciable part of the hyperons be scattered, the mean free path λ_s must be sufficiently short. An upper limit for λ_s can be set by the use of Fig. 11, where it is seen that for $\lambda_s = 10\lambda_{geom}$, for instance, only 20% of the Σ 's are scattered, a fraction that is negligible in the present connection. It can be estimated that if the value of α^+ / α^- is to be explained on the basis of scattering, then it is required that λ_s is shorter than about $3\lambda_{geom}$.⁵⁰ On the other hand, the present argument gives no lower limit for λ_s . Even if λ_s were so short that most hyperons would be scattered many times before reaching the surface and would arrive with very low kinetic energies, a value of V_Σ somewhat larger than -10 Mev can be found for which $g_{tr\Sigma^+} / g_{tr\Sigma^-}$ has the observed value.

It is, of course, not excluded that the difference between the ratios α^+ / α^- and $g_{tr\Sigma^+} / g_{tr\Sigma^-}$ is due to failure of the model. This would affect more strongly calculations for negative than for positive hyperons, because a larger part of the spectrum of Σ^- corresponds to negative energy states. The difference between the calculated and the observed ratios would tend to become smaller, if the effect of finite nuclear size were an increase in the fraction of hyperons created in negative energy states.⁵¹

(IV) So far, it has been assumed that charge-exchange scattering is negligible [although part of the considerations of (III) is independent of this assumption]. We now consider the alternative that charge-exchange scattering is important. This process increases the $\alpha^+ : \alpha^-$ ratio, as can be seen from fact, easily demonstrated on the assumption of charge independence, that in a self-conjugate nucleus the probability of charge-exchange is the same for Σ^+ , Σ^- , $\Sigma^0 \rightarrow \Sigma^+$ and $\Sigma^0 \rightarrow \Sigma^-$. Then, it follows from the production ratio (in nuclei) $\Sigma^- : \Sigma^0 : \Sigma^+ = 3:2:1$,³² that charge-exchange scattering tends to equalize the number of Σ^+ and of Σ^- . (The sum $\Sigma^+ + \Sigma^-$ remains unchanged.) Therefore, the ratio $(\Sigma^+ / \Sigma^-)_s$ of hyperons reaching the surface can approach the observed ratio. If, for instance, about one-half of the hyperons undergo charge-exchange scattering (λ_{ce} , as lengthened by the exclusion principle, about equal to $2.5\lambda_{geom}$), then the supply of Σ^+ is changed by a factor 1.5, and that of Σ^- by a factor $\frac{5}{3}$. This gives a ratio $(\Sigma^+ / \Sigma^-)_s = (1.5 \times 1) / (\frac{5}{3} \times 3) = 0.6$, only moderately less than the observed ratio 0.9. Of course, the calculated ratio would be closer to unity, if charge-exchange scattering were more frequent. It follows that in the present case the difference in the values of α^+ and α^- need not

⁵⁰ The limit given refers to the mean free path as lengthened by the effect of the exclusion principle. Correction for this effect would lower the limit. However, the correction factor would be closer to unity than the factor of ~ 0.5 , which one would obtain from the calculations of R. M. Sternheimer, [Phys. Rev. **106**, 1027 (1957)], because in the present situation the interest is mainly in the larger energy losses which are not so much inhibited by the exclusion principle.

⁵¹ Of course, the ratio α^+ / α^- would also be reduced, if the $\Sigma^- : \Sigma^+$ production ratio were less than 3:1.

be ascribed to the effect of the Coulomb potential, and, consequently, repulsive potentials are not ruled out by observation; instead, as will presently be shown, attractive potentials are less likely. (However, a repulsive potential is made unlikely by other considerations; see Sec. 8.)

It can easily be demonstrated that for Σ hyperons moving in a self-conjugate nucleus $\lambda_{ce} \gg \lambda_s$ for any choice of the scattering matrix elements of the isotopic spin states $T=\frac{1}{2}$ and $T=\frac{3}{2}$. Therefore, for each charge-exchange scattering there must have occurred at least one ordinary scattering process. This means that in the above-given example the majority of Σ 's reaching the surface must have been scattered. We can, then, use the earlier finding that for Σ 's scattered once and for $V_\Sigma \geq 0$ the ratio of the escape probabilities of Σ^+ and of Σ^- is ~ 2 . In the present case it is, then, expected that the observed ratio be $\Sigma^+/\Sigma^- \simeq 2 \times 0.6 = 1.2$ which is larger than the observed number 0.9.

(V) A lower limit for the absorption mean free path λ_a is obtained by ignoring the trapping of hyperons by a potential and attributing the reduction in the number of Σ 's entirely to absorption. (This situation could be realized, if V_Σ were less than -10 Mev. The difference between α^+ and α^- is now ignored.) Comparing the fraction 0.17 of events in which a charged hyperon is observed with the fraction 0.51 of K^- captures (see Sec. 6.1) in which such a particle is created, it is seen that 0.3 of the charged hyperons escape. Figure 11 shows that if the fraction escaping, g_i , is 0.3, then $\lambda_a = 1.5\lambda_{geom}$ for $\delta=0.2$, and $\lambda_a = 1.0\lambda_{geom}$ for $\delta=0.1$. If charge-exchange scattering is negligible, then a limit for λ_a can be similarly found from α^+ . For the lower experimental limit of α^+ , 0.46, this gives $\lambda_a = 3.7\lambda_{geom}$ for $\delta=0.2$ and $\lambda_a = 2.8\lambda_{geom}$ for $\delta=0.1$. (These limits do not disagree with the assumption made in Sec. 6.2 about the size of the reaction cross section.)

6.5 Abundance of Pions

Data given earlier can be used to explain the observed frequencies of groups C and D, that is, of the groups of events without charged hyperons, and, respectively, with and without pions. Charge-exchange scattering of pions will be neglected. Denoting the escape probability of pions by β , indicating the type of K^- -capture reaction by the end products, and using square brackets to symbolize frequencies, one gets for the frequency of group C the expression

$$[C] = \beta \{ (1 - \alpha^+) [\Sigma^+ + \pi^-] + (1 - \alpha^-) [\Sigma^- + \pi^+] + [\Sigma^0 + \pi^-] + [\Lambda^0 + \pi^-] \}. \quad (5)$$

We take $\beta=0.5$. For pions created in reaction (Ia), this value was found experimentally;⁵⁸ it is also the value obtained from Fig. 11 with the use of the pion-nucleon cross section, averaged over the pion spectrum of the reaction. Using our values of α^+ and α^- and the previously quoted relative reaction frequencies, one

obtains from Eq. (5) $[C]=0.24$, and, from a similar expression, $[D]=0.55$, in good agreement with the corresponding frequencies 0.26 and 0.51 listed in Table IV.⁶²

7. TRAPPING OF Λ^0 HYPERONS

7.1 Validity of the Model

In this section it will be discussed what information about the scattering of Λ^0 hyperons by nucleons can be drawn from the estimated number of trapped Λ^0 's, provided that the optical model is again used.

However, the validity of the model is more doubtful when it is applied to the trapping of Λ^0 's than in the previously discussed case of Σ hyperons, because for Λ^0 's there exists no strong absorptive reaction. Consequently, the discrete levels of Λ^0 's in negative-energy states are broadened only by transitions to lower-lying levels (energy gains of Λ^0 's are prevented by the exclusion principle, at least if the nucleus trapping the Λ^0 is in its ground state), and the lowest level is necessarily sharp. An estimate of the lifetime, and therefrom of the width, of the other levels, based in analogy to the argument in Sec. 6.2 on a comparison with the time it takes a particle moving in a nucleus to collide and be scattered, might be inaccurate, because the rate of transitions between discrete levels could be quite different from the rate of such collisions. As the results obtainable by the use of the optical model may, therefore, be unreliable, we shall present them and the steps involved in their derivation only in brief outline.

7.2 Numerical Data

To find from the fraction of events in which a Λ^0 is retained in a nucleus the fraction of Λ^0 's that is trapped, one needs the number of all Λ^0 's created, be it in the capture reaction (Ib) or in the transformation reaction (A). This number must equal the number of events in which no Σ , charged or neutral, escaped from the nucleus. The fraction of stars in which a charged Σ left the nucleus was found to be 0.17 (see Table IV). For Σ^0 , the nuclear well depth is $V=V_\Sigma$, the same as was used for Σ^+ in Sec. 6.3, and the fraction escaping is the same for Σ^0 as for Σ^+ , namely 0.61. As Σ^0 's are produced in about⁵³ 0.26 of all K^- captures (compare Sec. 6.1), a Σ^0 must have been emitted from $0.61 \times 0.26 = 0.16$ of all K^- captures. Thus, a Σ , charged or neutral, was emitted from $0.16 + 0.17 = 0.33$ of the stars. A Λ^0 was made in the nucleus in the remaining 0.67 of the captures, either directly by reaction (Ib) in 0.18 of the stars, or indirectly by transformation of a trapped Σ in 0.49 of the events. It is seen that the major source of Λ^0 's is reaction (A) which produces three-quarters of all Λ^0 's.

⁵² Strictly, the hyperfragment events, line 8 of Table IV, should be added to groups C and D, before the comparison with the calculated numbers is made.

⁵³ There is a minor uncertainty because the number of Σ^0 's from reaction (II) is not known.

Accepting the estimate of Sec. 5.4, we find that a Λ^0 is trapped either in the residual nucleus or in a hyperfragment in 0.14 of the stars (Table IV, line 10). This is a small fraction of the Λ^0 's created, namely $0.14/0.67=0.21$.

7.3 Outline of Calculations

Once the model is adopted, the discussion of the behavior of Λ^0 's in nuclei is simpler than that of Σ^0 's for two reasons. (a) The nuclear potential for Λ^0 , V_Λ , is not an unknown parameter, but can be estimated from the binding energies B_Λ of Λ^0 's in hyperfragments. From the trend of B_Λ with increasing atomic number⁵⁴ and from the calculations of Brown and Peskin,⁵⁵ we take $V_\Lambda=15$ Mev. (V_Λ could be larger by a few Mev, but hardly smaller.) (b) Only one type of strong Λ^0 -nucleon interactions, namely ordinary scattering, occurs.

The calculations are generally analogous to those concerning the trapping of Σ hyperons. As the majority of Λ^0 's result from reaction (A), computations were carried out for this process. In this case, the production spectrum is obtained by an integration over the four parameters characterizing an individual reaction: the initial nucleon energy T_F , the initial Σ energy T_Σ , the angle between the directions of motion of the nucleon and of the Σ , and the angle (in the c.m. system) between the direction of motion of the c.m. system and the direction of emission of the Λ^0 .⁵⁶ Isotropy in the c.m. system and a velocity-independent cross section were assumed for reaction (A). The possibility was ignored that the Σ 's may have been scattered before being transformed into Λ^0 's.

From the integral spectrum so derived, it was found that the fraction $f_{t\Lambda}$ (defined in analogy to the fraction $f_{i\Sigma}$ for Σ^0 's) of Λ^0 's trapped in a well 15 Mev deep is 0.04, considerably smaller than the observed trapping fraction.

It was to be expected that scattering of Λ^0 's within the nucleus could greatly increase the calculated trapping fraction. This effect was, therefore, investigated next. The spectrum of Λ^0 's that have been scattered once was calculated assuming again isotropy in the c.m. system and an energy-independent cross section. The effects of the exclusion principle, which reduces the number of collisions resulting in small energy gain of the nucleon and in small energy loss of the Λ^0 and which prevents energy gains of the Λ^0 , were taken into account. For the spectrum so derived, it was found that for $V_\Lambda=15$ Mev, the fraction of Λ^0 's of kinetic energy less than V_Λ is $f_{t\Lambda}'=0.20$, and the fraction reflected at the nuclear surface is $f_{r\Lambda}'=0.19$.

⁵⁴ L. M. Brown, Phys. Rev. **106**, 354 (1957).

⁵⁵ L. M. Brown and M. Peshkin, Phys. Rev. **107**, 272 (1957), and M. Peshkin (private communication).

⁵⁶ It would have been necessary to calculate the Σ spectrum in the same manner, if $V_K+V_C>0$.

A lower limit for the fraction of Λ^0 's trapped is obtained by multiplying the sum $(f_{t\Lambda}'+f_{r\Lambda}')=0.39$ by the probability, f_i , that a Λ^0 collides at least once before reaching the surface. (f_i is related to the previously defined escape probability g_i by the equation $f_i=1-g_i$.) Previously, f_i had been calculated for emulsion nuclei on the assumption that 0.6 of the processes considered occur in AgBr, and 0.4 in the light emulsion nuclei. In the present case, it is doubtful to what extent the light elements are effective in trapping a scattered Λ^0 , because it is possible that a light nucleus, excited by the processes mentioned in Sec. 5.4, has progressed considerably on the way to complete disintegration before the chain of events— K^- capture, Σ transformation, Λ^0 scattering, Λ^0 arrival at the surface—leading to Λ^0 trapping is completed. For use in the present context, therefore, f_i was computed as a function of the scattering mean free path λ_s for the case that only one-half of the light nuclei are effective (see Fig. 11, dashed curve). For the parameter δ (defined in Sec. 6.3), the median 0.2 was again selected. This is a good approximation, as the points of scattering, which is a tertiary process, should be much more uniformly distributed than the points of K^- capture considered in Sec. 6.3.

It remains to estimate λ_s . As the effect of the exclusion principle was already included in the calculation of the Λ^0 spectrum, the mean free path here required is that which is obtained by ignoring this principle. An upper limit for λ_s can be derived from an equation relating the potential to the real part of the forward-scattering amplitude for coherent scattering. If V_Λ is energy-independent and if the scattering is isotropic, then this limit is given by⁵⁷

$$\lambda_s \leq [1.1(m_\pi c)^4(m_N+m_\Lambda)^2/(m_N m_\Lambda V_\Lambda)^2] \lambda_{\text{geom}}. \quad (6)$$

For $V_\Lambda=15$ Mev one obtains $\lambda_s \leq 7\lambda_{\text{geom}}$. For this limit, one reads from the dashed curve of Fig. 11 that $f_i \geq 0.23$.

For the fraction of Λ^0 's trapped after scattering, one gets $f_i(f_{t\Lambda}'+f_{r\Lambda}') \geq 0.23 \times 0.39 = 0.09$. This limit is less than the observed fraction 0.20. However, the calculated result represents an underestimate, not only because the value of f_i used is a lower limit, but, mainly, because the effect of multiple scatterings was ignored.

This effect can in part be taken into account by considering that in subsequent scatterings the pa-

⁵⁷ Compare E. Fermi, [*Nuclear Physics* (University of Chicago Press, Chicago, 1950), revised edition, p. 201], and Frank, Gammel, and Watson [Phys. Rev. **101**, 891 (1956)]. It must be pointed out that this inequality is derived for positive particle energies and that the extension to negative energy states, implied by the use of the value of V_Λ found from hyperfragment binding, is doubtful. The use of relation (6) to determine the mean free path of Λ^0 's of kinetic energies larger than the well depth implies the assumption that V_Λ is the same for Λ^0 's in negative- and in positive-energy states. Some justification for this assumption comes from the observation that the dependence of Λ^0 binding energy on atomic number is consistent with a value of V_Λ that does not change when, with increasing nuclear size, the Λ^0 kinetic energy decreases.

parameter δ will again on the average be 0.2. Thus, the probability that after a series of collisions a Λ^0 is scattered again is still f_i . Ignoring reflections for the reason given in Sec. 6.3, and also ignoring for simplicity the further degradation of the Λ^0 spectrum in additional collisions, we obtain an improved estimate of the fraction f_Λ of Λ^0 's, trapped before collision or after one or more collisions, from the easily derived expression

$$f_\Lambda = f_{i\Lambda} + f_i f_{i\Lambda}' + f_i^2 (1 - f_{i\Lambda}') f_{i\Lambda}' + \dots \\ = f_{i\Lambda} + \frac{f_i f_{i\Lambda}'}{1 - f_i (1 - f_{i\Lambda}')} \quad (7)$$

Applying Eq. (7) separately to light and heavy emulsion nuclei (for which $f_i \geq 0.20$ and ≥ 0.32 , respectively) and averaging, one gets $f_\Lambda \geq 0.10$. Correction for reflections raises this limit to about 0.15.

This limit still represents a considerable underestimate for the following reasons. (a) Calculations were carried out for reaction (A). The Λ^0 's created in reaction (Ib) have originally a lower average energy and are, therefore, more readily trapped. (b) If part of the Σ hyperons were scattered and lost energy before being transformed into Λ^0 's, the Λ^0 spectrum would also be less energetic. (c) The values of f_i are lower limits. (d) The strong increase in trapping caused by the further degradation of the Λ^0 spectrum in the additional collisions was ignored.

It may be concluded that calculations based on the optical model and on the assumptions of energy independence and isotropy of the scattering process lead to a lower limit for the expected trapping fraction that is about equal to the observed fraction 0.20.

Of course, if the scattering mean free path were actually considerably shorter than the limit deduced from relation (6), the calculated trapping fraction could be much increased. Then, it would not be possible to assume simultaneously validity of the model, isotropy of the Λ -nucleon scattering, and an energy-independent scattering cross section.

8. SUMMARY

(a) Within an experimental error of 0.7%, the mass of K^- mesons is the same as that of τ^+ mesons; their lifetime agrees with the lifetime of positive mesons within the error of 40%. These findings are in accord with theoretical concepts.⁵⁸ K^- mesons are strongly interacting particles; in the kinetic-energy interval of 15–100 Mev they have a mean free path in emulsion about equal to the geometric.

(b) Observations on the capture of K^- mesons by nuclei are in agreement with the law of conservation of strangeness which demands that in such a capture a hyperon must be produced. Charged Σ hyperons were observed in 14% of the stars produced by K^- mesons

interacting at rest; in an additional 5% a hyperfragment was observed. From the data it is estimated that a Λ^0 was trapped in a nucleus without formation of a visible hyperfragment in 8% of the captures. In all events in which no hyperparticle was seen, the visible star-energy is sufficiently low so that a Λ^0 could have been emitted. In fact, the difference between the available energy of 494 Mev and the visible star energy E_{vis} is generally quite large: in events in which no pion is seen, E_{vis} averages about 60 Mev; pions carry away about 200 Mev in kinetic and rest energies. Even allowing for the energy of neutrons, it would be difficult to account for the missing energy, unless it is believed that part of it is consumed in the creation of an unstable particle, such as a Λ^0 .

(c) Of the K^- capture processes possible if strangeness is conserved, capture by a single nucleon resulting in the creation of a Σ hyperon and a pion (reaction Ia) occurs in about four-fifths of the events; the corresponding reaction in which a Λ^0 instead of a Σ is made (reaction Ib) takes place in about one-fifth of the interactions. A K^- is captured nonmesonically by two nucleons (reaction II) in roughly 5% of the events.

(d) Comparing the frequencies with which positive and negative hyperons are emitted from K^- capture stars with the creation frequencies, deduced on the assumption of charge independence from the observed abundance of reaction (Ib) and from the $\Sigma^-:\Sigma^+$ production ratio observed in a hydrogen bubble chamber,⁵² it is found that the ratio of the number of hyperons observed to the number created is $\alpha^+ = 0.61$ for Σ^+ and $\alpha^- = 0.24$ for Σ^- . These numbers are interpreted on the basis of an optical model.

Two alternative possibilities are considered, namely, first, that charge-exchange scattering of Σ hyperons in nuclei is negligible and, second, that it is a frequent process. In the first-named case, the reduction of the number of observed hyperons below the number created is at least in part attributed to the effect of an attractive potential V which prevents hyperons of kinetic energy less than the depth of the potential well from escaping from the nucleus. The difference between α^+ and α^- can then be explained as an effect of the Coulomb potential ($V_C = 3$ Mev for light emulsion nuclei, $V_C = 10$ Mev for AgBr) which deepens the well for negative hyperons. It is, furthermore, found that, in the absence of charge-exchange scattering, the above-given values of α^+ and α^- exclude a repulsive nuclear potential stronger than 10 Mev, and limit an attractive potential, V_Σ , to values less than 20 Mev. (This result agrees with a conclusion of Capps⁵⁹ who also used the optical model to analyze the data of Gilbert *et al.*¹⁹.) The quantities α^+ and α^- are best fitted, if Σ hyperons in nuclear matter had a mean free path for ordinary scattering less than 3 times the geometric and if there existed an attractive potential V_Σ of about 10 Mev.

⁵⁸ G. Lüders and B. Zumino, Bull. Am. Phys. Soc. Ser. II, 2, 190 (1957).

⁵⁹ R. H. Capps, Phys. Rev. 107, 239 (1957).

In the second-named case, the difference between α^+ and α^- can be explained as an effect of charge-exchange scattering which can be shown to increase the supply of positive hyperons and decrease that of negative hyperons. In this case, a repulsive potential is favored.

On the basis of the data so far mentioned, a choice between the two alternatives is not possible. However, if the nuclear potential is repulsive, one should find few positive hyperons of kinetic energy less than $|V_c + V_\Sigma|$.

Our own sample of hyperons is too small to construct a reliable hyperon spectrum, although it can be seen from Table V that the Σ^+ kinetic energy can be as low as 10 Mev. However, the more extensive data of Fry *et al.*¹⁶ and of Gilbert *et al.*¹⁹ show that the Σ^+ spectrum extends down to ~ 5 Mev. Thus it follows that a repulsive nuclear potential can be excluded. The second alternative, strong charge-exchange scattering, is, therefore, less likely.⁶⁰ This implies that the mean free path for charge-exchange scattering in a nucleus is appreciably larger than 3 times geometric.

It can also be shown that in the absence of charge-exchange scattering, the mean free path for absorption of Σ hyperons must be larger than 3 times geometric.

(e) If the capture of Λ^0 hyperons in nuclei is computed on the basis of the optical model, assuming an energy-independent and isotropic Λ^0 -nucleon scattering cross section, it is found that a lower limit for the calculated fraction of trapped Λ^0 's is close to the observed fraction.

APPENDIX

(A1) Total Reflection

If a potential is zero at the left side of a boundary, and V on the right side, and the kinetic energy of a particle is T on the left side, then the angle of total reflection φ_t is determined by

$$\sin \varphi_t = (1 - V/T)^{1/2}. \quad (8)$$

The angle φ_t is independent of the *shape* of the potential step.

Let a particle be emitted from a point P located a distance d from the surface of a sphere of radius r . Let the angle of emission relative to the radius through P be ϑ ; then ϑ is related to the angle of incidence φ at the

⁶⁰ Unless the Σ^+/Σ^- production ratio in nuclei is appreciably larger, say ≥ 5 , than the ratio 3 previously used (see Sec. 6).

surface by

$$\sin \varphi = (1 - d/r) \sin \vartheta. \quad (9)$$

Let ϑ_t correspond to φ_t . Upon combining Eqs. (8) and (9), and considering that the fraction reflected R equals the fraction of particles emitted into the solid angle between ϑ_t and $\pi - \vartheta_t$ which for isotropic emission equals $\cos \vartheta_t$, Eq. (4) is obtained.

(A2) Fraction Colliding

Let the definitions of (A1) be used, let x be the length of a trajectory from P to the surface, and let λ be the mean free path. Then the fraction reaching the surface without colliding is

$$g_i = \frac{1}{2} \int_{-1}^{+1} \exp(-x/\lambda) d(\cos \vartheta). \quad (10)$$

Expressing x in terms of r , d , and ϑ , and performing the integration, one obtains, with $\delta = d/r$ and $\eta = r/\lambda$,

$$g_i = [4\eta(1-\delta)]^{-1} \{ [1 + 2\eta(1-\frac{1}{2}\delta)] \exp(-\eta\delta) - [1 + \eta\delta] \exp[-2\eta(1-\frac{1}{2}\delta)] - 2\eta^2\delta(1-\frac{1}{2}\delta) \times [\text{Ei}(-2\eta(1-\frac{1}{2}\delta)) - \text{Ei}(-\eta\delta)] \}, \quad (11)$$

where Ei is the exponential integral. The fraction colliding is $f_i = 1 - g_i$. The curves in Fig. 11 were calculated by evaluating Eq. (11) separately for the radii r of light and of heavy emulsion nuclei, defining λ_{geom} as explained in reference 49.

ACKNOWLEDGMENTS

We are most deeply indebted to Dr. E. O. Salant for his great interest in and generous support of this work. We have much profited by long discussion with Dr. J. W. Cronin, Dr. B. H. McCormick, Dr. K. McVoy, and Dr. R. Serber. The research could not have been done without the conscientious and efficient work at the microscope of M. R. Bracker, B. M. Cozine, J. J. Grant, J. Greener, A. C. Lea, J. D. Leek, B. B. Lowe, E. R. Medd, E. C. Phillips, G. F. Smith, R. H. Wagner, and in particular, M. C. Hall, who also rendered invaluable aid in the compilation of the data. J. W. Quinn and J. E. Smith were of great assistance in the experimental work. Finally, we gratefully acknowledge the unfailing cooperation of the Cosmotron staff and the kindness of Dr. E. J. Lofgren who arranged the exposure at the Bevatron.